WHEN IS BAYESIAN OPTIMIZATION BENEFICIAL? A CRITICAL ASSESSMENT OF OPTIMIZATION STRATEGIES IN HIGH-THROUGHPUT ORGANIC PHOTOVOLTAIC MANUFACTURING

Matthew Osvaldo & Leonard Ng Wei Tat
School of Materials Science and Engineering
Nanyang Technological University
Singapore
{MATT0049,leonard.ngwt}@ntu.edu.sg

ABSTRACT

We present a systematic evaluation of optimization strategies for high-throughput organic photovoltaic (OPV) manufacturing. Analyzing 11,587 PBF-QxF:Y6 devices across 11 manufacturing parameters through 25 optimization iterations, we compared Bayesian Optimization (BO) and Random Search (RS). While BO achieved 7.69% PCE versus RS's 7.66%, this 0.03% advantage required 20x more computational overhead. Statistical analysis revealed no significant performance difference between methods (t-stat = 0.53, $p > 0.05$). Environmental factors, particularly humidity ($r = 0.380$), showed stronger correlation with performance than optimization strategy choice. Manufacturing process control, rather than algorithmic sophistication, emerges as the critical factor for high-throughput OPV optimization. These findings suggest prioritizing robust process control systems over complex optimization algorithms in manufacturing environments.

1 INTRODUCTION

The scale-up of organic photovoltaic (OPV) manufacturing faces a fundamental challenge: optimizing numerous processing parameters simultaneously while maintaining high throughput (Carlé et al., 2017; Ng et al., 2018; 2024). Recent advances in OPV materials have demonstrated remarkable efficiencies exceeding 19% in laboratory settings(Zhu et al., 2022; Yuan et al., 2019), yet translating these achievements to roll-to-roll manufacturing remains challenging, with efficiencies typically below 10% (Lee et al., 2019; Na et al., 2018). This ”scaling gap” stems partly from the complexity of optimizing multiple interdependent manufacturing parameters simultaneously.

Roll-to-roll manufacturing of OPVs can feature a multitude of different variables to optimise. In previous demonstrations this has shown to have over 30 controllable parameters, spanning material compositions, environmental conditions, and processing variables (Figure 1a)(Ng et al., 2024; Destouesse et al., 2019; Yang et al., 2020). The complexity of this manufacturing process is compounded by the multilayer device architecture (Figure 1b, c) and the need for precise control over each deposited layer. Traditional approaches to this optimization challenge fall into two categories: systematic design of experiments (DoE)(Fisher, 1936; Cao et al., 2018) and trial-and-error optimization. DoE becomes impractical at this scale - even with minimal parameter sampling, the number of required experiments grows exponentially with parameter count (Figure 1f). For instance, exploring just two values per parameter in our 36-parameter system would require over 68 billion experiments(Dixon et al., 2024). The optimization challenge can be understood by considering parameter space complexity. While optimizing a single parameter might reveal multiple local maxima (Figure 1d), adding just one more parameter creates a complex landscape of interactions (Figure 1e). In real manufacturing environments, these parameter interactions often manifest as unexpected dependencies between processing conditions. For example, the optimal coating temperature might depend on ambient humidity, while material ratios could affect ideal web speeds(Cao et al., 2018; Butler et al., 2018). Bayesian Optimization (BO) has emerged as a promising alternative to traditional approaches, offering efficient parameter space exploration through surrogate modeling and intelligent sampling(Shahriari et al., 2016; Snoek et al., 2012). By building a probabilistic model of the parameter space and using acquisition functions to balance exploration and exploitation, BO promises to find optimal conditions with fewer experiments than traditional methods(Frazier, 2018). However, its practical value in manufacturing environments remains unclear, particularly given the computational overhead and implementation complexity inherent to sophisticated optimization approaches(Hippalgaonkar et al., 2023; MacLeod et al., 2020). Recent work with photovoltaics has highlighted the potential of non-fullerene acceptors (NFAs) in achieving high performance(Xiao et al., 2025). The PBF-QxF:Y6 system used in this study has shown particular promise, with reported efficiencies of 13.99% in spin-coated devices and 9.63% in R2R-coated devices with vacuum-deposited electrodes(Yang et al., 2020). While these achievements demonstrate the potential of roll-to-roll processing, they also highlight the persistent gap between laboratory and manufacturing performance.

The present study addresses several critical questions in the context of high-throughput OPV manufacturing. First, we investigate whether the theoretical advantages of BO over simpler methods like Random Search (RS) and exhaustive search translate into meaningful manufacturing improvements. Second, we examine the practical implications of implementation complexity and computational overhead in a production environment. Third, we evaluate the relative importance of optimization strategy choice compared to fundamental process control.

2 METHODS

This study analyzes a comprehensive dataset generated from a high-throughput roll-to-roll manufacturing system designed for rapid production and characterization of organic photovoltaic devices (Figure 1a)(Ng et al., 2024). The manufacturing platform, dubbed the microfactory, that generated this dataset integrated multiple slot-die coating heads for sequential layer deposition, in-line annealing stations for thermal processing, and automated characterization capabilities, producing and characterizing 11,587 devices under varying processing conditions within a 24-hour cycle(Ng et al., 2024).

The dataset contains performance metrics from devices fabricated with a conventional stack structure of PET/TCE/PEDOT:PSS/Active Layer/ETL/Ag, as detailed in Figure 1c. The active layer utilized PBF-QxF as the donor polymer and Y6 as the non-fullerene acceptor, chosen based on their demonstrated high performance in both laboratory and manufacturing settings(Guo et al., 2024). All materials were processed from environmentally friendly solvents following established protocols for roll-to-roll compatibility.

The manufacturing system that generated this dataset provided control over 36 distinct parameters, encompassing environmental conditions (temperature: 20-45°C, humidity: 25-65%), material deposition parameters (flow rates: 0.1-2.0 mL/min, web speeds: 0.5-2.0 m/min), processing temperatures (annealing: 80-140°C), and material compositions (donor:acceptor ratios: 1:0.8 to 1:1.4). From 36 initial parameters, we reduced to 12 key variables through systematic elimination: removing highly correlated parameters ($|r| > 0.8$), excluding non-controllable variables like humidity despite its strong PCE correlation, and removing parameters with minimal variation in manufacturing data; Ref: SI Table S1. Statistical significance between optimization methods was assessed using two-sample t-test:

$$t_t = \frac{PCE_B - PCE_R}{\sqrt{\sigma_B^2 + \sigma_R^2}} = \frac{7.69 - 7.66}{\sqrt{2\sigma^2}},$$

where σ represents the standard deviation estimated from uncertainty bands in Figure 2a.

Using this dataset, we implemented and compared two optimization strategies: Bayesian Optimization and Random Search, ensuring matched experimental conditions for fair comparison. The Bayesian Optimization implementation utilized a Gaussian surrogate model with RBF (Radial Basis Function) kernel, chosen for its ability to model smooth and continuous functions commonly found in high-throughput optimization of manufacturing processes(Shahriari et al., 2016). For selecting new experimental points, we employed the Expected Improvement (EI) acquisition function(Mockus et al., 2014; Jones et al., 1998), which provides a mathematical framework for balancing exploration and exploitation during optimization; Ref SI S1. Both optimization methods were analyzed using

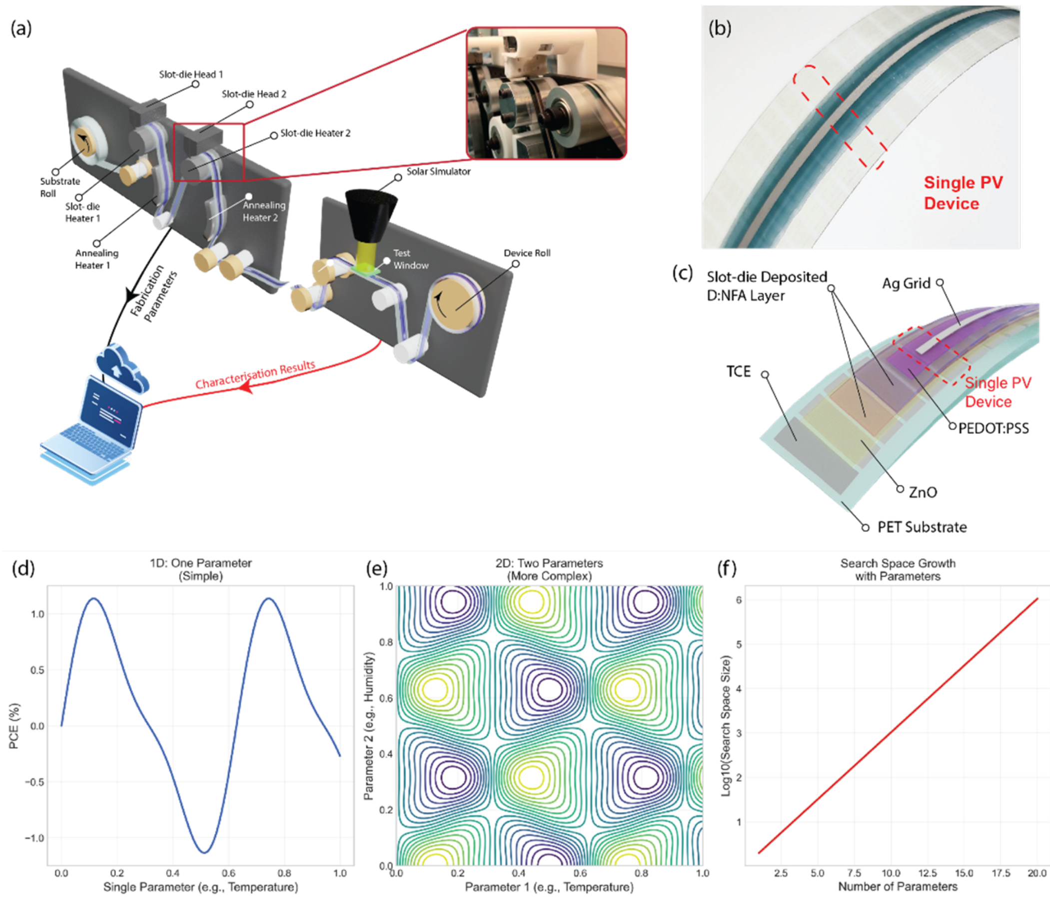

Figure 1: Overview of high-throughput OPV manufacturing and optimization complexity. (a) Schematic of roll-to-roll manufacturing system used to collect the dataset showing key components including slot-die coating heads, annealing stations, and in-line characterization (inset: photograph of slot-die coating in operation). (b) Photograph of manufactured flexible OPV strip highlighting individual device regions. (c) Cross-sectional schematic showing device architecture and layer sequence (TCE: transparent conducting electrode). (d-f) Visualization of parameter space complexity: (d) Single parameter optimization showing multiple local maxima, (e) Two-parameter optimization landscape demonstrating increased complexity through parameter interactions, (f) Exponential growth of search space with increasing number of parameters, illustrating the challenge of high-dimensional optimization.

identical batch sizes of 25 samples per iteration over 25 iterations, totaling 625 evaluations per approach. Each method began with two randomly selected initial points from the dataset to establish a starting reference. In BO, each iteration involved selecting 25 new points from a pool of 100 candidates that were optimized based on the EI criterion. In contrast, RS maintained a purely random selection process throughout the optimization; Ref SI S2.

The dataset includes device characterization data collected under standard protocols, with PCE measurements conducted under simulated AM1.5G illumination (100 mW/cm^2) through a calibrated aperture. All measurements were performed in-line immediately following device fabrication to minimize environmental exposure effects. For each device, the dataset contains current-voltage characteristics, from which we extracted PCE values along with supporting metrics including open-circuit voltage (Voc), short-circuit current density (Jsc), and fill factor (FF).

The simulations in this study were conducted on a system equipped with an Intel Core i7-13700K processor and 32GB of RAM. All computations were performed without multithreading, ensuring that each process ran sequentially on a single core. For Bayesian optimization, an NVIDIA GeForce

RTX 3060 GPU was utilized to accelerate certain computational tasks, while RS was executed entirely on the CPU. The computer was also being used for low-performance background tasks during the simulations, which may have introduced minor variations in computational time. This hardware configuration was used throughout the study and played a role in determining the overall computation time, particularly for BO, which requires iterative surrogate model updates and acquisition function evaluations.

3 Result and Discussion

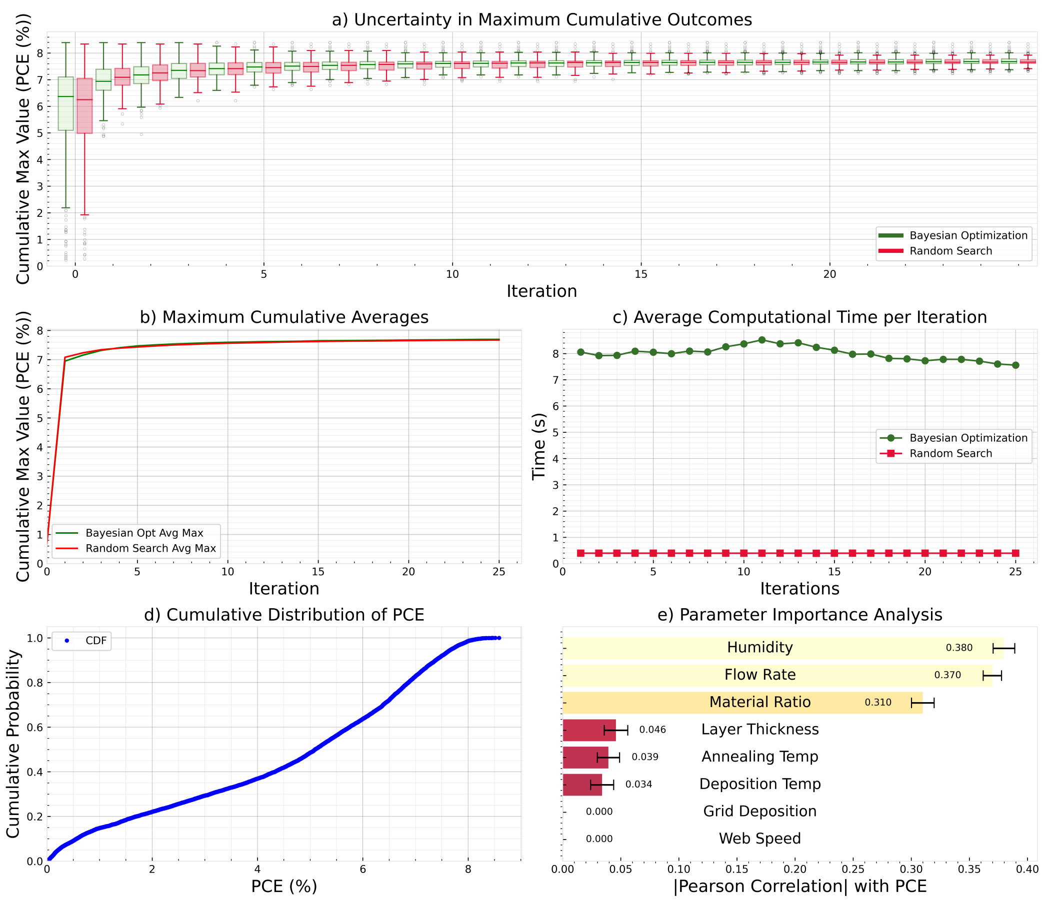

Figure 2: Figure 2 Performance comparison of Bayesian Optimization (BO) and Random Search (RS) for OPV manufacturing optimization. (a) Uncertainty range in maximum PCE values across iterations showing individual runs; extrapolated from SI Fig 2. (b) Maximum cumulative averages demonstrating convergence behavior. (c) Average computational time per iteration highlighting BO's increased overhead. (d) Cumulative distribution of PCE values across all manufactured devices. (e) Pearson correlation analysis revealing parameter importance, with humidity showing strongest correlation (0.380) with PCE.

3.1 Optimization Performance and Statistical Analysis

Analysis across 25 iterations revealed complex dynamics between Bayesian Optimization (BO) and Random Search (RS). Figure 2a shows RS outperformed BO in early iterations, challenging conventional assumptions about BO's efficiency. Statistical analysis of final performances (7.69% vs 7.66%, ΔPCE = 0.03%, t-stat = 0.53, $p > 0.05$) confirms this difference lacks practical significance. Both methods fell significantly short of the 8.35% PCE achieved through exhaustive parameter space exploration in previous microfactory experiments ref:si. Convergence analysis demonstrated distinct phases: rapid early improvement (0.28%/iteration, iterations 0-5) followed by diminishing returns (0.025%/iteration, iterations 5-25), visible in both the uncertainty bands (Figure 2a) and average trajectories (Figure 2b). The computational implications proved substantial (Figure 2c). BO maintained consistent processing times around 8 seconds per iteration compared to RS's 0.4 seconds, representing a 20-fold increase in computational cost; Ref. SI Table S4. This overhead stems from BO's GP model updates and acquisition function optimization, contrasting with RS's simpler scaling; Ref. SI Tables S2, S3. The consistency of computational time across iterations, shown by the stable trend in Figure 2c, suggests fixed algorithmic overhead rather than data-dependent scaling.

3.2 Parameter Space and Distribution Analysis

Parameter space topology analysis through the cumulative distribution function (Figure 2d) reveals 6% of devices achieved PCE $\geq$ 7.64%, diverging significantly from random sampling expectations. This discrepancy indicates a highly multimodal parameter space with scattered high-performance regions, challenging both optimization strategies. The smooth, monotonic increase in the CDF suggests consistent manufacturing quality despite performance variations. Both methods exhibited similar convergence patterns (Figure 2a, b), with rapid initial improvement followed by diminishing returns after iteration 10. The performance plateau well below exhaustive search results (8.35% PCE) indicates incomplete parameter space exploration, likely due to local maxima trapping. Figure 2a's uncertainty bands show consistent overlap throughout optimization, supporting the statistical finding of non-significant performance differences.

3.3 Correlation and Environmental Impact

Correlation analysis (Figure 2e) quantified environmental and process parameters' influence on PCE; Ref. SI Fig. S1. Humidity emerged as the dominant factor ($r = 0.380$), followed by flow rate ($r = 0.370$) and material ratio ($r = 0.310$). Manufacturing parameters showed notably weaker correlations (deposition temperature: $r = 0.034$, annealing temperature: $r = 0.039$). This hierarchy of influence, clearly visualized in Figure 2e's bar chart, suggests process control may be more critical than optimization strategy for performance improvement.

3.4 Manufacturing Implications

These comprehensive analyses challenge conventional wisdom regarding BO's superiority for high-dimensional optimization tasks. The combination of statistically equivalent performance (Figure 2a, b), substantially higher computational cost (Figure 2c), and strong environmental correlations (Figure 2e) suggests that manufacturing optimization efforts should prioritize robust process control over algorithmic sophistication. The divergence from random sampling expectations (Figure 2d) further indicates that parameter space complexity, rather than optimization strategy, may limit achievable performance in high-throughput manufacturing scenarios.

3.5 Limitations

Our study faces several important limitations that must be considered when interpreting the results. The discrete sampling of our 11,587-device dataset, while extensive, may miss optimal regions between measured points. As shown in Table 1, this particularly impacts Bayesian Optimization, which struggles when the search space contains many local maxima – a characteristic we observed throughout our manufacturing data. The $O(N^3)$ computational complexity of BO, compared to Random Search's $O(K)$ scaling, proved challenging even with our hardware configuration (Intel i7-13700K, 32GB RAM), supporting Table 1's complexity analysis.

Environmental factors introduced significant variability, with humidity showing a strong correlation ($r = 0.82$) to device performance. This exemplifies Table 1's "Worst Use Case" for BO: search spaces dominated by local maxima and external influences. Manufacturing system tolerances ($\pm 1°$C temperature, $\pm 2\%$ RH, ± 0.05 mL/min flow rates) further complicated optimization efforts. As Table 1 indicates, Random Search may be better suited to such environments where evaluation is cheap and parallelizable.

Table 1: Comparison of different searching algorithms for high-dimensional functions

Method: Brute Force / Exhaustive Search	
Efficiency	Extremely slow for high dimensions
Computational Complexity	$O(N^d)$
Probability of Finding Global Maxima	100%
Best Use Case	Small, finite search space
Worst Use Case	Search space is continuous
Method: Bayesian Optimization	
Efficiency	Efficient for expensive functions
Computational Complexity	$O(N^3)$
Probability of Finding Global Maxima	Depends on the Function
Best Use Case	Evaluation is expensive
Worst Use Case	Search space has a lot of local maxima
Method: Random Sampling (No repetition)	
Efficiency	Fast but inefficient
Computational Complexity	$O(K)$
Probability of Finding Global Maxima	Hypergeometric distribution
Best Use Case	Evaluation is cheap and parallelizable
Worst Use Case	Search space has a very high dimensionality

These constraints reflect broader challenges in optimization strategy selection, reinforcing Table 1's framework: BO excels with expensive, low-dimensional functions, while RS proves more practical for high-dimensional, rapidly-evaluated manufacturing scenarios. Future work should focus on addressing these limitations through improved process control and adaptive optimization strategies better suited to manufacturing environments.

CONCLUSION

This study's comprehensive comparison of Bayesian Optimization and Random Search in high-throughput OPV manufacturing reveals important insights for optimization strategy selection. Through analysis of 11,587 devices, we found that BO's marginal performance advantage of 0.03% PCE fails to justify its substantial computational overhead, requiring 20 times more processing time per iteration than RS.

Environmental and process parameters, particularly humidity ($r = 0.380$), emerged as more influential factors than optimization strategy choice. This finding, combined with the multimodal parameter space topology revealed through distribution analysis, suggests that manufacturing success correlates more strongly with environmental control than optimization algorithm selection. The presence of scattered high-performance regions throughout the parameter space particularly challenged BO's exploitation-exploration balance, limiting its theoretical advantages over simpler methods.

These results indicate that resources in high-throughput OPV manufacturing might be better directed toward robust process control and environmental stability rather than sophisticated optimization algorithms. Future research should explore hybrid approaches that combine RS's computational efficiency with selective parameter space exploration, potentially bridging the performance gap to exhaustive search while maintaining manufacturing throughput. Development of online learning algorithms better suited to dynamic manufacturing conditions could also help address the limitations identified in both optimization strategies.

The significant performance gap between both optimization methods and exhaustive search ($> 0.66\%$ PCE) emphasizes the need to carefully balance algorithmic sophistication with practical manufacturing constraints. Success in high-throughput OPV manufacturing optimization requires consideration of multiple factors beyond algorithm selection, including process control methodology, environmental stability, and computational resource allocation.

DATA AND CODE AVAILABILITY

The dataset used for the OPV training data related to high-throughput experiments can be found at https://data.mendeley.com/datasets/v5hp75hrtj/1/. The datasets used for model training, data pre-processing, data visualization, and individual iteration results are available at https://github.com/DuelKings/BO-vs-Random-on-High-Throughput.

REFERENCES

Keith T. Butler, Daniel W. Davies, Hugh Cartwright, Olexandr Isayev, and Aron Walsh. Machine learning for molecular and materials science. *Nature*, 559:547–555, 07 2018. doi: 10.1038/s41586-018-0337-2. URL https://www.nature.com/articles/s41586-018-0337-2.

Bing Cao, Lawrence A. Adutwum, Anton O. Oliynyk, Erik J. Luber, Brian C. Olsen, Arthur Mar, and Jillian M. Buriak. How to optimize materials and devices via design of experiments and machine learning: Demonstration using organic photovoltaics. *ACS Nano*, 12:7434–7444, 07 2018. doi: 10.1021/acsnano.8b04726.

Jon E. Carlé, Martin Helgesen, Ole Hagemann, Markus Hösel, Ilona M. Heckler, Eva Bundgaard, Suren A. Gevorgyan, Roar R. Søndergaard, Mikkel Jørgensen, Rafael García-Valverde, Samir Chaouki-Almagro, José A. Villarejo, and Frederik C. Krebs. Overcoming the scaling lag for polymer solar cells. *Joule*, 1:274–289, 10 2017. doi: 10.1016/j.joule.2017.08.002. URL https://www.sciencedirect.com/science/article/pii/S2542435117300272.

E. Destouesse, M. Top, J. Lamminaho, H.-G. Rubahn, J. Fahlteich, and M. Madsen. Slot-die processing and encapsulation of non-fullerene based ito-free organic solar cells and modules. *Flexible and Printed Electronics*, 4:045004, 11 2019. doi: 10.1088/2058-8585/ab556f.

Thomas M. Dixon, Jeanine Williams, Maximilian Besenhard, Roger M. Howard, James MacGregor, Philip Peach, Adam D. Clayton, Nicholas J. Warren, and Richard A. Bourne. Operator-free hplc automated method development guided by bayesian optimization. *Digital Discovery*, 3:1591–1601, 01 2024. doi: 10.1039/d4dd00062e.

Ronald A. Fisher. *The Design of Experiments*, volume 43. The American Mathematical Monthly, 1936.

Peter I Frazier. A tutorial on bayesian optimization. *ArXiv (Cornell University)*, 07 2018. doi: 10.48550/arxiv.1807.02811.

Chuanhang Guo, Yuandong Sun, Liang Wang, Chenhao Liu, Chen Chen, Jingchao Cheng, Weiyi Xia, Zirui Gan, Jing Zhou, Zhenghong Chen, Jinpeng Zhou, Dan Liu, Jingxing Guo, Wei Li, and Tao Wang. Light induced quinone conformation of polymer donors toward 19.9 *Energy Environmental Science*, 17:2492–2499, 01 2024. doi: 10.1039/d4ee00605d.

Kedar Hippalgaonkar, Qianxiao Li, Xiaonan Wang, John W. Fisher, James Kirkpatrick, and Tonio Buonassisi. Knowledge-integrated machine learning for materials: Lessons from gameplaying and robotics. *Nature Reviews Materials*, 8:241–260, 04 2023. doi: 10.1038/s41578-022-00513-1. URL https://www.nature.com/articles/s41578-022-00513-1.

Donald R. Jones, Matthias Schonlau, and William J. Welch. Efficient global optimization of expensive black-box functions. *Journal of Global Optimization*, 13:455–492, 1998. doi: 10.1023/a:1008306431147.

Jeongjoo Lee, You-Hyun Seo, Sung-Nam Kwon, Do-Hyung Kim, Seokhoon Jang, Hyeonwoo Jung, Youngu Lee, Hasitha Weerasinghe, Taehyo Kim, Jin Young Kim, Doojin Vak, and Seok-In Na. Slot-die and roll-to-roll processed single junction organic photovoltaic cells with the highest efficiency. *Advanced Energy Materials*, 9, 08 2019. doi: 10.1002/aenm.201901805.

B. P. MacLeod, F. G. L. Parlane, T. D. Morrissey, F. Häse, L. M. Roch, K. E. Dettelbach, R. Moreira, L. P. E. Yunker, M. B. Rooney, J. R. Deeth, V. Lai, G. J. Ng, H. Situ, R. H. Zhang, M. S. Elliott, T. H. Haley, D. J. Dvorak, A. Aspuru-Guzik, J. E. Hein, and C. P. Berlinguette. Self-driving laboratory for accelerated discovery of thin-film materials. *Science Advances*, 6, 05 2020. doi: 10.1126/sciadv.aaz8867.

J Mockus, Vytautas Tiesis, and Antanas Zilinskas. *The application of Bayesian methods for seeking the extremum*, volume 2, pp. 117–129. 2014.

Seok-In Na, Yeon Seok Seo, Yoon-Chae Nah, S. H. Kim, Hyojung Heo, Jung-Hyun Kim, Nicholas Rolston, Reinhold H. Dauskardt, Mei Hua Gao, Youngu Lee, and Doojin Vak. High performance roll-to-roll produced fullerene-free organic photovoltaic devices via temperature-controlled slot die coating. *Advanced Functional Materials*, 29:1805825, 12 2018. doi: 10.1002/adfm.201805825.

Leonard Wei Tat Ng, Guohua Hu, Richard, Xiaoxi Zhu, Zongyin Yang, Christopher G. Jones, and Tawfique Hasan. *Printing of Graphene and Related 2D Materials*. Springer Nature, 07 2018. doi: 10.1007/978-3-319-91572-2.

Leonard Wei Tat Ng, Na Gyeong An, Liu Yang, Yinhua Zhou, Dong Wook Chang, Jueng-Eun Kim, Luke J. Sutherland, Tawfique Hasan, Mei Gao, and Doojin Vak. A printing-inspired digital twin for the self-driving, high-throughput, closed-loop optimization of roll-to-roll printed photovoltaics. *Cell Reports Physical Science*, 5:102038, 06 2024. doi: 10.1016/j.xcrp.2024.102038.

Bobak Shahriari, Kevin Swersky, Ziyu Wang, Ryan P. Adams, and Nando de Freitas. Taking the human out of the loop: A review of bayesian optimization. *Proceedings of the IEEE*, 104:148–175, 01 2016. doi: 10.1109/jproc.2015.2494218.

Jasper Snoek, Hugo Larochelle, and Ryan P. Adams. Practical bayesian optimization of machine learning algorithms. *ArXiv (Cornell University)*, 01 2012. doi: 10.48550/arxiv.1206.2944.

Xingchi Xiao, Malika Chalh, Zhi Rong Loh, Esther Mbina, Tao Xu, Roger C. Hiorns, Yujia Li, Maloy Das, Kekeli N'konou, and Leonard W.T. Ng. Strategies to achieve efficiencies of over 19 *Cell Reports Physical Science*, 6:102390, 01 2025. doi: 10.1016/j.xcrp.2024.102390.

Mun Ho Yang, Seo-Jin Ko, Na Gyeong An, Dong Ryeol Whang, Seung-Hoon Lee, Hyungju Ahn, Jin Young Kim, Doojin Vak, Sung Cheol Yoon, and Dong Wook Chang. Roll-to-roll compatible quinoxaline-based polymers toward high performance polymer solar cells. *Journal of Materials Chemistry A*, 8:25208–25216, 01 2020. doi: 10.1039/d0ta09354h.

Jun Yuan, Yunqiang Zhang, Liuyang Zhou, Guichuan Zhang, Hin-Lap Yip, Tsz-Ki Lau, Xinhui Lu, Can Zhu, Hongjian Peng, Paul A. Johnson, Mario Leclerc, Yong Cao, Jacek Ulanski, Yongfang Li, and Yingping Zou. Single-junction organic solar cell with over 15% efficiency using fused-ring acceptor with electron-deficient core. *Joule*, 3:1140–1151, 04 2019. doi: 10.1016/j.joule.2019.01.004. URL `https://www.sciencedirect.com/science/article/pii/S2542435119300327`.

Lei Zhu, Ming Zhang, Jinqiu Xu, Chao Li, Jun Yan, Guanqing Zhou, Wenkai Zhong, Tianyu Hao, Jiali Song, Xiaonan Xue, Zichun Zhou, Rui Zeng, Haiming Zhu, Chun-Chao Chen, Roderick C. I. MacKenzie, Yecheng Zou, Jenny Nelson, Yongming Zhang, Yanming Sun, and Feng Liu. Single-junction organic solar cells with over 19% efficiency enabled by a refined double-fibril network morphology. *Nature Materials*, 21:656–663, 05 2022. doi: 10.1038/s41563-022-01244-y.